

## ELECTROCHEMISTRY OF L-NIOBIUM PENTOXIDE IN A LITHIUM/NON-AQUEOUS CELL\*

TSUTOMU OHZUKU\*\* and KEIJIRO SAWAI

*Electrochemistry and Inorganic Chemistry Laboratory, Department of Synthetic Chemistry, Faculty of Engineering, Okayama University, Okayama 700 (Japan)*

TAKETSUGU HIRAI

*Industrial Inorganic Chemistry Laboratory, Department of Applied Chemistry, Faculty of Engineering, Osaka City University, Sugimoto 3-3-138, Sumiyoshi, Osaka 558 (Japan)*

(Received September 2, 1986)

### Summary

The electrochemical behaviour of L-Nb<sub>2</sub>O<sub>5</sub> (orthorhombic;  $a = 6.162$ ,  $b = 3.661$ ,  $c = 3.919$  Å) was examined in a 1 M LiClO<sub>4</sub>-propylene carbonate/tetrahydrofuran (1:1) solution at 30 °C. L-Nb<sub>2</sub>O<sub>5</sub> exhibited an S-shaped discharge curve (mid-point about 1.58 V) under a low, continuous drain below 5 mA g<sup>-1</sup> without addition of any conductive binder (such as graphite or acetylene black) and it could be reduced up to 2 F mol<sup>-1</sup>. The performance of Li/Nb<sub>2</sub>O<sub>5</sub> cells was examined: these were found to belong to the 1.5 V class of lithium cell at both low and high discharge rates.

The reaction mechanism of L-Nb<sub>2</sub>O<sub>5</sub> in a lithium/non-aqueous cell was investigated by *ex situ* X-ray diffraction analysis together with a chronopotentiometric technique. Reversibility tests indicated that the reaction of L-Nb<sub>2</sub>O<sub>5</sub> was basically reversible over 0 - 2 F mol<sup>-1</sup> of reduction, which agreed with the analytical results of *ex situ* XRD studies. The electrochemistry of L-Nb<sub>2</sub>O<sub>5</sub>, especially the characteristic S-shaped electrode potential curve, is discussed in terms of a homogeneous phase reaction.

---

### Introduction

Insertion electrodes are of considerable interest to battery researchers. The term "insertion electrode" generally refers to an electrode system into which foreign ions can be inserted during an electrochemical reduction process. Insertion electrodes can be divided into two categories: (i) that involving a homogeneous (single) phase reaction; (ii) that giving a two-

---

\*Part of this work was presented at the 3rd International Meeting on Lithium Batteries, Kyoto, Japan, May 27 - 30, 1986.

\*\*Author to whom correspondence should be addressed.

phase reaction. The term "topotactic" is used to represent those electrochemical reactions that can proceed without destroying the skeleton structure of the material.

Recently, niobium pentoxide ( $\text{Nb}_2\text{O}_5$ ) has been investigated [1, 2] as a cathode material for non-aqueous cells. Pure  $\text{Nb}_2\text{O}_5$  is inherently an insulator and is white in colour because the  $\text{Nb}^{5+}$  ion has no d-electrons. The electrochemical behaviour of  $\text{Nb}_2\text{O}_5$ , however, has not been examined in detail, especially in relation to its crystal structure.

In a previous paper [3], we discussed a solid-state redox reaction which proceeds in a homogeneous phase, and proposed an analytical expression for the characteristic S-shaped curve in the electrode potential *versus* degree of reduction plots, emphasizing the role of charge carriers. Although the electrochemical reduction of L-niobium pentoxide ( $\text{L-Nb}_2\text{O}_5$ ) proceeds in a homogeneous phase (as will be reported here), the shape of the electrode potential *versus* degree of reduction plots deviates from an ideal S-shaped curve.

The objectives of the present paper are to understand the reaction mechanism of  $\text{L-Nb}_2\text{O}_5$  in a lithium/non-aqueous cell in relation to the crystal structure of  $\text{L-Nb}_2\text{O}_5$ , and to discuss possible causes for the non-ideal behaviour of electrode potential *versus* degree of reduction plots.

## Experimental

Niobium pentoxide was obtained from Nakarai Chemical Co., Ltd. and was used "as received". The sample was characterized by X-ray diffraction (XRD) and BET surface area measurements. The XRD measurements were performed using a Shimadzu Model XD-3A X-ray diffractometer, both with copper  $K\alpha$  radiation filtered with nickel and with iron  $K\alpha$  radiation filtered with manganese. The BET surface area of the sample was examined using a Monosorp Model SA-1000 instrument (Shibata Scientific Co., Ltd.).

Each experimental cell consisted of a lithium anode (15 mm  $\times$  20 mm) and an  $\text{Nb}_2\text{O}_5$  cathode (15 mm  $\times$  20 mm) separated by a sheet of polypropylene non-woven cloth (FT-330, Bylean Japan). The preparation methods were the same as those described previously [4]. Conductive binders such as acetylene black, carbon black or graphite were used only in reversibility tests. The prepared cathodes were dried under vacuum at 150 °C before use. All cell construction procedures were carried out in a dry box.

The electrolyte was 1 M  $\text{LiClO}_4$ -propylene carbonate/tetrahydrofuran (1:1) solution containing less than 100 mg  $\text{l}^{-1}$  of water. All electrochemical measurements were carried out at 30 °C. Departures from the above experimental conditions are described, where appropriate, in later sections of the paper.

TABLE 1

Analysis of XRD data of Nb<sub>2</sub>O<sub>5</sub> (orthorhombic;  $a = 6.162$ ,  $b = 3.661$ ,  $c = 3.919$  Å)

No.	$d_{\text{obs}}$	$I_{\text{obs}}$	( $h, k, l$ )	$d_{\text{calc}}$	$I_{\text{calc}}^*$	( $h, k, l$ )	$d_{\text{calc}}$	$I_{\text{calc}}^{**}$
1	5.214	5	—	—	—	(1, 3, 0)	5.211	6
2	3.926	100	(0, 0, 1)	3.916	100	(0, 0, 1)	3.916	100
3	3.470	6	—	—	—	(1, 7, 0)	3.462	3
4	3.403	4	—	—	—	—	—	—
5	3.145	88	(1, 1, 0)	3.147	96	(1, 8, 0)	3.147	92
6	3.083	46	(2, 0, 0)	3.081	56	(2, 0, 0)	3.081	38
7	2.717	5	—	—	—	(2, 5, 0)	2.727	2
8	2.457	51	(1, 1, 1)	2.454	42	(1, 8, 1)	2.454	42
9	2.425	23	(2, 0, 1)	2.422	26	(2, 0, 1)	2.422	17
10	2.121	6	—	—	—	(2, 10, 0)	2.123	1
						(1, 13, 0)	2.116	2
11	2.009	12	(2, 1, 1)	2.020	2	(2, 11, 0)	2.015	1
						(3, 3, 0)	2.010	4
12	1.966	29	(0, 0, 2)	1.960	21	(0, 0, 2)	1.960	21
13	1.829	30	(0, 2, 0)	1.831	16	(0, 16, 0)	1.831	11
14	1.791	30	(3, 1, 0)	1.791	24	(3, 8, 0)	1.791	16
15	1.663	57	(1, 1, 2)	1.664	27	(1, 8, 2)	1.664	26
			(0, 2, 1)	1.659	15	(0, 16, 1)	1.659	11
			(2, 0, 2)	1.653	15	(2, 0, 2)	1.653	11
16	1.629	14	(3, 1, 1)	1.629	21	(3, 8, 1)	1.629	15
17	1.572	13	(2, 2, 0)	1.574	15	(2, 16, 0)	1.574	10
18	1.540	8	(4, 0, 0)	1.541	7	(4, 0, 0)	1.541	2
19	1.461	17	(2, 2, 1)	1.460	12	(2, 16, 1)	1.460	10
20	1.433	6	(4, 0, 1)	1.434	8	(1, 13, 2)	1.438	1
						(4, 0, 1)	1.434	2
						(4, 1, 1)	1.432	1
21	1.337	11	(0, 2, 2)	1.338	13	(0, 16, 2)	1.338	9
22	1.323	16	(3, 1, 2)	1.322	20	(3, 8, 2)	1.322	13
23	1.304	2	(0, 0, 3)	1.306	4	(0, 0, 3)	1.306	4

\*Calculation made assuming space group  $D_{1h}^2-Pmmm$ : Nb<sup>5+</sup> ions in 1(a) and 1(f) sites, O<sup>2-</sup> ions in 1(c), 1(b), 1(h) and 2(k) sites with oxygen parameter  $x = 0.2$ .

\*\*Calculation made on the basis of an orthorhombic unit cell [8] ( $a = 6.162$ ,  $b = 3.661 \times 8$ ,  $c = 3.919$  Å) using equivalent atomic positions with 15Ta<sub>2</sub>O<sub>5</sub>·2WO<sub>3</sub> (plane group  $Pm$ ) assuming no O(21) in ref. 11.

## Results

### Characterization of Nb<sub>2</sub>O<sub>5</sub> sample

The Nb<sub>2</sub>O<sub>5</sub> used was white in color with a resistivity larger than 10<sup>8</sup> ohm cm and a BET surface area below 3 m<sup>2</sup> g<sup>-1</sup>. X-ray diffraction data of the sample are summarized in the first column of Table 1. Niobium pentoxide has several modifications that have been denoted by the letters  $\alpha$ ,  $\beta$ ,  $\gamma$ ,  $\epsilon$ ,  $\delta$  or LL(TT), L(T), B, M, H, N, P (or I, II, III), by various authors [5]. Such nomenclature proposals are rather confusing. Observed  $d$ -values

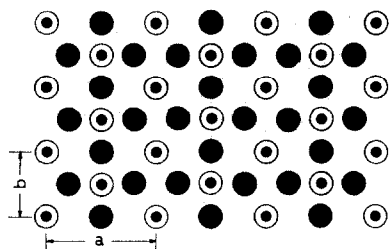


Fig. 1. Idealized crystal structure of L-Nb<sub>2</sub>O<sub>5</sub> (orthorhombic,  $a = 6.162$ ,  $b = 3.661$ ,  $c = 3.919$  Å; space group  $D_{2h}^1$ - $Pmmm$ ) projected on the (0,0,1) plane. Small and large circles indicate Nb<sup>5+</sup> and O<sup>2-</sup>, respectively, at  $z = 0$  (filled) and  $z = 0.5$  (open).

may be assigned assuming an orthorhombic unit cell having  $a = 6.162$ ,  $b = 3.661$  and  $c = 3.919$  Å, which may correspond to L-Nb<sub>2</sub>O<sub>5</sub> [5] or  $\gamma$ -Nb<sub>2</sub>O<sub>5</sub> [6]. In this paper we use the nomenclature L-Nb<sub>2</sub>O<sub>5</sub> as a designation of the form; this was first used by Brauer [7] and was also recommended by Schäfer *et al.* [5]. The letter T indicates the (low)-temperature form. Consequently, L-Nb<sub>2</sub>O<sub>5</sub> is equivalent to T-Nb<sub>2</sub>O<sub>5</sub> [8].

The crystal structure of L-Nb<sub>2</sub>O<sub>5</sub> is still unknown [5]. By ignoring minor peaks, we have calculated the unit cell volume to be 88.4 Å<sup>3</sup>. This suggests that the unit cell contains one formula unit of Nb<sub>2</sub>O<sub>5</sub>. We have considered idealized structures for L-Nb<sub>2</sub>O<sub>5</sub> based on the NbO<sub>6</sub>-octahedral linkage in H-Nb<sub>2</sub>O<sub>5</sub> [9] and M-Nb<sub>2</sub>O<sub>5</sub> [10]; the results are shown in Table 1. Integrated intensities have been calculated for an idealized structure by assuming the space group  $D_{2h}^1$ - $Pmmm$  (Nb<sup>5+</sup> ions in 1(a) and 1(f) sites; O<sup>2-</sup> ions in 1(c), 1(b), 1(h) and 2(k) sites with  $x = 0.2$ ). It can be seen (Table 1) that the calculated intensities are in good agreement with those observed for the sample, except for minor peaks.

In an idealized structure for L-Nb<sub>2</sub>O<sub>5</sub>, two types of NbO<sub>6</sub> octahedra are linked together by sharing edges and corners; they may be symbolized by (NbO<sub>4/3</sub>O<sub>2/2</sub>) octahedra and (NbO<sub>2/3</sub>O<sub>4/2</sub>) octahedra. (NbO<sub>4/3</sub>O<sub>2/2</sub>) octahedra are joined by two opposite edges with the neighbouring octahedra forming a chain of (NbO<sub>4/3</sub>O<sub>2/2</sub>) octahedra. (NbO<sub>2/3</sub>O<sub>4/2</sub>) octahedra are also joined by two opposite corners with neighbouring octahedra to form a chain of (NbO<sub>2/3</sub>O<sub>4/2</sub>) octahedra. Both chains are linked to one another in parallel by sharing corners. The resulting sheets of octahedra are connected by sharing corners to produce an idealized structure in which the Nb atoms are almost hexagonally arranged (Fig. 1).

Waring *et al.* [8] have proposed a crystal structure for L-Nb<sub>2</sub>O<sub>5</sub> (orthorhombic;  $a = 6.199$ ,  $b = 29.124$ ,  $c = 3.938$  Å) by analogy with the crystal structure of 15Ta<sub>2</sub>O<sub>5</sub>·2WO<sub>3</sub> [11] (orthorhombic;  $a = 6.172$ ,  $b = 29.226$ ,  $c = 3.850$  Å). Reflection indices based on an orthorhombic unit cell ( $a = 6.162$ ,  $b = 3.661 \times 8$ ,  $c = 3.919$  Å) and intensities calculated assuming no O(21) [11] and plane group  $Pm$  [8] are also shown in Table 1. Although almost every observed peak can be indexed, a crystal structure for L-Nb<sub>2</sub>O<sub>5</sub> based on that of 15Ta<sub>2</sub>O<sub>5</sub>·2WO<sub>3</sub> is complicated, especially in regard to the oxygen positions, because of the necessary removal of O(21)

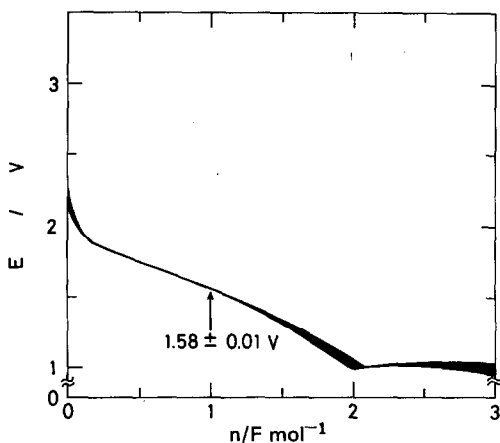


Fig. 2. Continuous discharge curve of an Li/L-Nb<sub>2</sub>O<sub>5</sub> cell at a discharge current below 5 mA g<sup>-1</sup>. No conductive binder in the cathode.

in the crystal structure of 15Ta<sub>2</sub>O<sub>5</sub>·2WO<sub>3</sub> [11]. Such a crystal structure can be made from the ideal crystal structure of L-Nb<sub>2</sub>O<sub>5</sub> (Fig. 1) by distorting the octahedra. In other words, the idealized crystal structure of L-Nb<sub>2</sub>O<sub>5</sub> may be an idealized sublattice of L-Nb<sub>2</sub>O<sub>5</sub>, proposed by Waring *et al.* [8].

Since the major peaks are equally well reproduced by both structural models for L-Nb<sub>2</sub>O<sub>5</sub>, an idealized crystal structure of L-Nb<sub>2</sub>O<sub>5</sub> (space group: *D*<sub>2h</sub><sup>1</sup>-*Pmmm*) having an orthorhombic unit cell (*a* = 6.162, *b* = 3.661, *c* = 3.919 Å), corresponding to the most simple form of the modifications of Nb<sub>2</sub>O<sub>5</sub>, is used in this paper for the purpose of structural description.

#### Continuous discharge curves at low rate

Figure 2 shows the continuous discharge curve of the Li/L-Nb<sub>2</sub>O<sub>5</sub> cell at a low rate (below 5 mA g<sup>-1</sup> of L-Nb<sub>2</sub>O<sub>5</sub>). The weight of L-Nb<sub>2</sub>O<sub>5</sub> was varied from 10 to 50 mg. The degree of reduction, *n*, in F mol<sup>-1</sup>, was calculated from the discharge capacity and the moles of L-Nb<sub>2</sub>O<sub>5</sub> used. The blocked-in area indicates the scatter of the results. Since no conductive binders were used, the working voltage at about 1 V is not due to the decomposition of the solvent. Such a low voltage discharge is not dealt with in this paper.

Figure 2 shows that the Li/L-Nb<sub>2</sub>O<sub>5</sub> cell has a distorted S-shaped discharge curve, with a mid-point at 1.58 ± 0.01 V, and that L-Nb<sub>2</sub>O<sub>5</sub> is able to be reduced up to 2 F mol<sup>-1</sup> in a lithium/non-aqueous cell.

#### Pulse-discharge curve at intermediate rate

In order to examine whether or not L-Nb<sub>2</sub>O<sub>5</sub> is a suitable active material for intermediate and/or heavy duty use, a high current pulse was applied to an Li/L-Nb<sub>2</sub>O<sub>5</sub> cell. The result is shown in Fig. 3; the open-circuit voltage curve agrees well with the low-rate discharge curve observed above (Fig. 2).

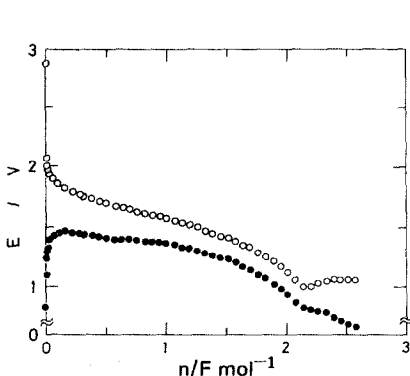


Fig. 3. Pulse discharge curve (10 s on, 80 s off) of an Li/L-Nb<sub>2</sub>O<sub>5</sub> cell. Cathode: L-Nb<sub>2</sub>O<sub>5</sub>, 27.3 mg (no conductive binder). Current: 3 mA/3 cm<sup>2</sup> (corresponding to 110 mA g<sup>-1</sup>).

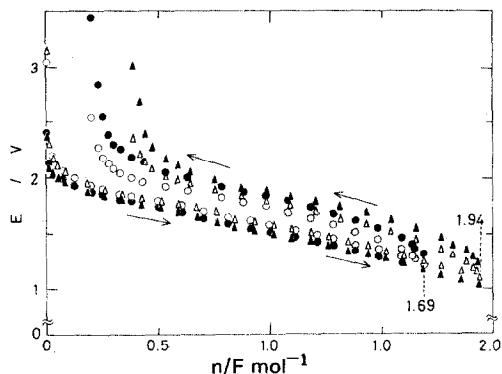


Fig. 4. Reversibility test results of an Li/L-Nb<sub>2</sub>O<sub>5</sub> cell. Cathode mix: L-Nb<sub>2</sub>O<sub>5</sub> (48 wt.%), acetylene black/graphite (1:1; 38 wt.%), Teflon (14 wt.%). Current pulse (20 s on, 80 s off for discharge; 10 s on, 80 s off for charge): 4 mA/3 cm<sup>2</sup>.

Thus, Figs. 2 and 3 demonstrate that L-Nb<sub>2</sub>O<sub>5</sub> may be applied to an active material for the 1.5 V class of lithium cell without addition of any conductive binders.

### Reversibility tests

In order to understand whether or not the observed S-shaped curve was the reversible potential of the Li/L-Nb<sub>2</sub>O<sub>5</sub> system, reversibility tests were carried out. In these tests, conductive binder and organic binder were used to give sufficient transmission lines and mechanical strength to the cathode and to minimize electrical isolation of active material during the charging process. Cells were discharged with a 4 mA pulse (20 s on, 80 s off) to a given depth of discharge and then charged with a 4 mA pulse (10 s on, 80 s off).

The results (Fig. 4) show that the electrochemical reaction of L-Nb<sub>2</sub>O<sub>5</sub> in a lithium/non-aqueous cell is reversible. The shapes of the open-circuit voltage curves obtained for the discharge and the charge processes indicate that the distorted S-shaped curves observed in electrochemical tests are close to the equilibrium voltage curves for the reaction taking place in the Li/L-Nb<sub>2</sub>O<sub>5</sub> cell.

### Ex situ XRD measurements

In order to examine changes in the crystal structure of L-Nb<sub>2</sub>O<sub>5</sub> during discharge, XRD measurements (using iron K $\alpha$  radiation filtered with manganese) were carried out on L-Nb<sub>2</sub>O<sub>5</sub> samples discharged at a low current density (5 mA g<sup>-1</sup>) to various depths of discharge. Polyethylene film was used to prevent the oxidation of these samples by oxygen and moisture present in the air during XRD measurements.

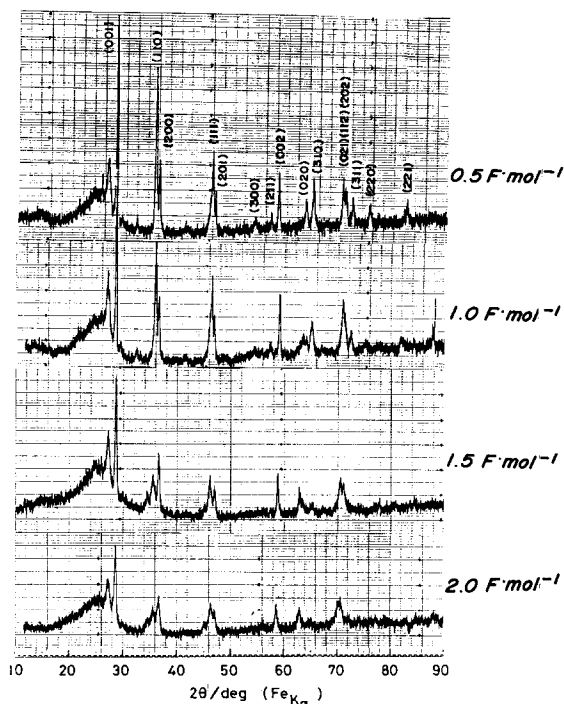


Fig. 5. X-ray diffraction data for reduced forms of L-Nb<sub>2</sub>O<sub>5</sub>.

The XRD results are presented in Fig. 5. Indices ( $h, k, l$ ) have been assigned on the basis of an orthorhombic unit cell ( $a = 6.162$ ,  $b = 3.661$ ,  $c = 3.919$  Å). At  $0.5 F \text{ mol}^{-1}$  of reduction, almost every major diffraction line of L-Nb<sub>2</sub>O<sub>5</sub> is observed. On further reduction, the diffraction lines broaden, especially (1,1,0), (1,1,1) and (3,1,0), and some lines are hardly recognized as peaks at  $2 F \text{ mol}^{-1}$  of reduction. Although line shapes are broader than those of the original L-Nb<sub>2</sub>O<sub>5</sub>, major peaks, such as (0,0,1), (1,1,0), (2,0,0), (1,1,1), (2,0,1), (0,0,2), (0,2,0), (0,2,1), (1,1,2), and (2,0,2), survive even at  $2 F \text{ mol}^{-1}$  of reduction. Among these, the position of the (0,2,0) line shifts to a lower diffraction angle, *i.e.*, the  $d$ -value changes from 1.829 Å to 1.853 Å, corresponding to a change in the  $b$  axis of the orthorhombic unit cell from 3.661 Å to 3.705 Å at  $2 F \text{ mol}^{-1}$  of reduction. From these XRD data, we conclude that the reduction of L-Nb<sub>2</sub>O<sub>5</sub> in a lithium/non-aqueous cell is a topotactic reaction.

At all levels of reduction up to  $2 F \text{ mol}^{-1}$ , the original L-Nb<sub>2</sub>O<sub>5</sub> could be recovered by subjecting the reduced samples to either electrochemical or chemical oxidation.

#### Performance of laboratory cells

The above findings indicate that the Li/L-Nb<sub>2</sub>O<sub>5</sub> couple offers promise for the development of a 1.5 V class of lithium cell if a characteristic S-

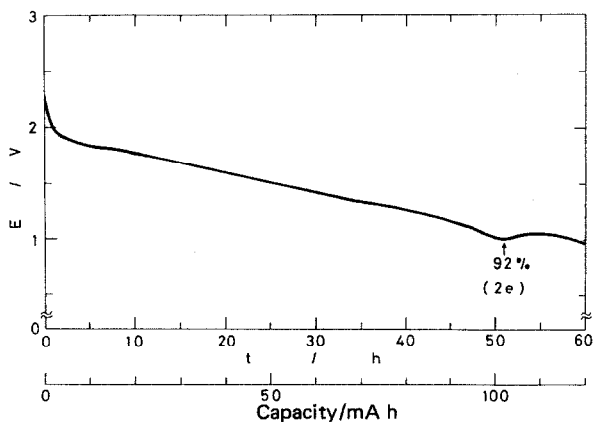


Fig. 6. Discharge curve of an Li/L-Nb<sub>2</sub>O<sub>5</sub> cell at 2 mA. Cathode: 0.551 g L-Nb<sub>2</sub>O<sub>5</sub>, no conductive binder.

shaped curve is an advantage in its application. In order to confirm the applicability of the cell, cells having 100 - 150 mA h capacities were fabricated and examined. Each cell consisted of two lithium anodes (15 mm × 20 mm) and an L-Nb<sub>2</sub>O<sub>5</sub> cathode (15 mm × 15 mm). The cathodes were prepared by pressing a dry L-Nb<sub>2</sub>O<sub>5</sub> powder on a 100 mesh stainless steel screen with a frame of titanium (1 mm thick, 4 mm wide) having a spot-welded terminal wire. The amount of electrolyte used was 0.5 ml. Figure 6 shows the typical discharge behaviour of these cells and the data demonstrate that the Li/L-Nb<sub>2</sub>O<sub>5</sub> cell without addition of conductive binder performs reasonably well. The average working voltage was found to be in the 1.5 - 1.6 V range. Thus, we conclude that Li/L-Nb<sub>2</sub>O<sub>5</sub> can be used as a 1.5 V class of lithium cell.

## Discussion

### *Reaction mechanism*

Both the X-ray diffraction and electrochemical data described above indicate that the electrochemical reaction of L-Nb<sub>2</sub>O<sub>5</sub> is a topotactic (single phase) process. Reichman and Bard [1] have reported a two-phase potential region at about 1.7 V (corresponding to the formation of LiNb<sub>2</sub>O<sub>5</sub>) until the reduction degree  $x$  in Li <sub>$x$</sub> Nb<sub>2</sub>O<sub>5</sub> reaches 1.5, followed by a single-phase region (formation of non-stoichiometric Li <sub>$x$</sub> Nb<sub>2</sub>O<sub>5</sub>). The sample of these authors was prepared on Nb metal by oxidizing the substrate in air at 550 °C; it had  $d$ -values of 3.16, 2.47, 2.13, 1.97, 1.83, 1.57 and 1.47 Å and seems to represent undeveloped  $\delta$ -Nb<sub>2</sub>O<sub>5</sub> (hexagonal;  $a = 3.62$ ,  $c = 3.93$  Å) [6] with the exception of the line  $d = 2.13$  Å. Disagreement between these data and the results of the present study are therefore due to the different crystal structure used for Nb<sub>2</sub>O<sub>5</sub>. A reversible character for Nb<sub>2</sub>O<sub>5</sub> has also

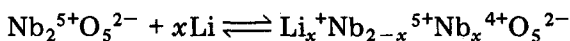


been reported by Kumagai and Tanno [2], who prepared samples by a two-stage oxidation of Nb metal powder in a secondary lithium cell. Our results agree well with those of this latter study in that there is a full-range of reversibility.

The ideal structure of  $\text{L-Nb}_2\text{O}_5$  has the orthorhombic space group  $Pmmm$  with  $\text{Nb}^{5+}$  ions (octahedral sites) at positions 1(a) and 1(f) and  $\text{O}^{2-}$  ions at positions 1(c), 1(b), 1(h) and 2(k) (with positional parameter  $x = 0.2$ ) as shown in Fig. 1. Thus  $\text{L-Nb}_2\text{O}_5$  does not have close-packed oxygen ions in its crystal lattice. Consequently, there are several vacant sites between hexagonally arranged niobium sheets. When electrons are inserted into the structure,  $\text{Nb}^{5+}$  ions ( $d^0$ ) at positions 1(a) and/or 1(f) are converted to  $\text{Nb}^{4+}$  ions ( $d^1$ ) at the same positions. Electrons on  $\text{Nb}^{4+}$  ions can move between 1(a) and 1(f) sites with the aid of thermal energy and an external electric field. Excess charge may be compensated by the accommodation of  $\text{Li}^+$  ions into vacant sites available between the hexagonally arranged niobium sheets.  $\text{Li}^+$  ions may also be mobile between these sites (2-dimensional channel). Thus, the partially reduced  $\text{L-Nb}_2\text{O}_5$  is both an electron and an ion conductor. This may be the reason why conductive binders are not required in the construction of cathodes for an  $\text{Li/L-Nb}_2\text{O}_5$  cell.

The  $\text{Li}^+$  ions are distributed statistically in the free space between niobium sheets and may interact with each other. A large population of  $\text{Li}^+$  ions may contribute to structural disorder due to the electrostatic interaction between these ions and the Nb-O lattice. A microscopic distribution of  $\text{Li}^+$  ions may induce short-range disorder. For example,  $\text{O}^{2-}$  ions at 1(c) and 1(h) sites in Fig. 1 may deviate from their regular positions, dependent on the detailed location of  $\text{Li}^+$  ions. Since  $\text{L-Nb}_2\text{O}_5$  has hexagonally arranged niobium sheets, such a distortion is more likely to occur along the (1,1,0) rather than along the (0,0,1) plane. The short-range disorder discussed above may affect the XRD peak profiles, but not the location of the peaks, as shown in Fig. 5.

From these considerations, the following topotactic (single phase) reaction mechanism is proposed for the electrochemical reaction of  $\text{L-Nb}_2\text{O}_5$  in a lithium/non-aqueous cell.



Orthorhombic

$$\begin{bmatrix} a = 6.162 \\ b = 3.661 \\ c = 3.919 \text{ \AA} \end{bmatrix}$$

Orthorhombic

$$\begin{bmatrix} a = 6.16\bar{2} \\ b = 3.70\bar{5} \\ c = 3.91\bar{9} \text{ \AA} \end{bmatrix}$$

$$(0 < x < 2)$$

where the  $\text{Nb}^{5+/4+}$  ions are located in 1(a) and 1(f) sites,  $\text{O}^{2-}$  ions in 1(c), 1(b), 1(h) and 2(k) sites in space group  $Pmmm$ , and the  $\text{Li}^+$  ions are distributed statistically between hexagonally arranged niobium sheets.

### Characteristic S-shaped discharge curve

The situation described in the previous section is characteristic for a solid-state redox reaction that proceeds in a homogeneous phase by inserting foreign ions. In a previous paper [3], the difference between a redox electrochemical reaction in a solution phase and that in a solid phase was discussed, and an analytical expression was proposed for a characteristic S-shaped discharge curve in the electrode potential ( $E$ ) versus the degree of reduction ( $y$ ) plots for an ideal solid-state redox reaction in a homogeneous phase.

If the condition required for applying the analytical expression reported previously [3] was applied to the  $\text{Li}_y\text{NbO}_{2.5}$  system ( $\text{Li}_x\text{Nb}_2\text{O}_5$  system), the  $E$  versus  $y$  plots must obey the equation:

$$E = E'_0 - \frac{2RT}{F} \ln \frac{y}{1-y} \quad (1)$$

where

$$E'_0 = E_0 + \frac{RT}{F} \ln a_{\text{Li}^+}$$

and  $y$  is the mole fraction of  $\text{Nb}^{4+}$  ions in the solid matrix.

However, the observed curve is much steeper than that calculated from eqn. (1).

In the earlier study [3], the ion-ion interaction in a solid matrix was not considered. In the case of the  $\text{Li}/\text{Nb}_2\text{O}_5$  homogeneous phase system,  $\text{Li}^+-\text{Li}^+$  ion interaction is likely to exist in a solid matrix due to the nature of the  $\text{L-Nb}_2\text{O}_5$  structure (*i.e.* an open structure in terms of lithium ion insertion). Because of this, the energy required to put an  $\text{Li}^+$  ion into an available site in a solid matrix is not the same for subsequent steps, since this depends on the  $\text{Li}^+$  ion concentration in a solid matrix.

The problem may be reduced to that of solving a partition function  $Z_{\text{Li}}$  for the  $\text{Li}^+$  ion:

$$Z_{\text{Li}} = \sum_{\alpha} \exp(-E_{\alpha}/kT) \quad (2)$$

where  $\Sigma_{\alpha}$  is an assembly of the state  $\alpha$  and  $E_{\alpha}$  is a total interaction energy [12, 13]. Although eqn. (2) for a cooperative system is difficult to solve rigorously in a general form, there are several solutions that can be obtained for special cases. To this end, an interaction energy can be formulated, based on a structural model, as follows.

If  $n_0$  sites are available for  $\text{Li}^+$  ion accommodation in a unit area at square planar lattice sites, the average distance ( $\bar{l}_{\text{site}}$ ) between this site and its neighbouring site can be expressed as

$$\bar{l}_{\text{site}} = \frac{1}{\sqrt{n_0}} \quad (3)$$

Similarly, if  $n$  sites per unit area are occupied by  $\text{Li}^+$  ions in the same square planar lattice, the average distance ( $\bar{l}$ ) between two neighbouring  $\text{Li}^+$  ions is:

$$\bar{l} = \frac{1}{\sqrt{n}} \quad (4)$$

Then, using eqns. (3) and (4), the electrostatic energy  $\phi$  for a pair of  $\text{Li}^+$  ions can be obtained from:

$$\phi = \frac{e^2}{4\pi\epsilon\bar{l}_{\text{site}}} \sqrt{y} \quad (5)$$

where  $y = n/n_0$  is the ratio of occupied sites and available sites. Consequently, the total electrostatic interaction energy as a function of  $y$  can be represented as:

$$E_c = \frac{Ae^2}{4\pi\epsilon\bar{l}_{\text{site}}} y^{3/2} \quad (6)$$

where  $A$  is a constant that can be obtained by geometry.

The partition function of  $\text{Li}^+$  ions for such a case can be expressed simply by:

$$Z_{\text{Li}} = \frac{n_0!}{n! (n_0 - n)!} \exp(-E_c/kT) \quad (7)$$

where  $E_c$  is given by eqn. (6).

By applying the usual formula to obtain the free energy,  $G(n)$ , and some approximations, the following equation can be derived, after converting the variable  $n$  to  $y$ ,

$$G(y) = \frac{Ae^2}{4\pi\epsilon\bar{l}_{\text{site}}} y^{3/2} + n_0 kT [y \ln y + (1 - y) \ln(1 - y)] \quad (8)$$

The first term in eqn. (8) corresponds to the enthalpy of the electrostatic interaction of  $\text{Li}^+$  ions, and the second term corresponds to the entropy for ideal mixing.

By calculating  $(1/n_0)(\partial G(y)/\partial y)$  and considering the effect of the electronic term [3], an expression for the electrode potential  $E$  as a function of  $y$  can be derived:

$$E = E'_0 - \frac{RT}{F} \left\{ 2 \ln \frac{y}{1-y} + \frac{u}{kT} y^{1/2} \right\} \quad (9)$$

where  $u$  is an interaction energy ( $3Ae^2/8\pi n_0 \epsilon \bar{l}_{\text{site}} > 0$ , *i.e.*, repulsion). In order to obtain eqn. (9), it is assumed that the available electron sites are equal to the number of available  $\text{Li}^+$  ions. Then,  $y$  in eqn. (9) corresponds to the mole fraction of  $\text{Nb}^{4+}$  ions in a solid matrix. By comparing eqns. (1) and (9), it is clear that the third term in eqn. (9) provides the degree of deviation from ideality due to the electrostatic interaction of  $\text{Li}^+$  ions. In other words, eqn. (9) reduces to eqn. (1) when there is no interaction between  $\text{Li}^+$  ions in the system, *i.e.*,  $u = 0$  in eqn. (9).

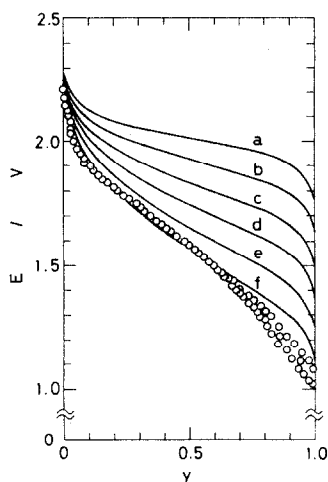


Fig. 7. Discharge curves for Li/L-Nb<sub>2</sub>O<sub>5</sub> system. Solid curves calculated from eqn. (9) (see text) with several  $u$ -values: (a) 0, (b) 5, (c) 10, (d) 15, (e) 20 and (f) 25  $kT$  assuming  $E'_0 = 2.02$  V.

Figure 7 shows the  $E$  versus  $y$  plots for the Li/L-Nb<sub>2</sub>O<sub>5</sub> system, together with the calculated curves from eqn. (9) with several  $u$ -values, assuming  $E'_0 = 2.02$  V. The effect of the interaction energy,  $u$ , on the distortion of the ideal S-shaped curve can be seen in Fig. 7. Since the degree of fit between the observed curve and the calculated curve with  $u = 25 kT$  is reasonably good within experimental error, it is concluded that the electrochemical reaction of L-Nb<sub>2</sub>O<sub>5</sub> in a lithium/non-aqueous cell is a thermodynamically "homogeneous phase" reaction in spite of the fact that the shape of the electrode potential plot is far from ideal.

The above arguments on the effect of ion-ion interactions in a solid matrix on an electrode potential are based on electrostatic interactions among square planar lattice sites, *i.e.*, 2-dimensional interactions. One can, however, easily extend the fundamental concept to an electrostatic interaction in linear lattice sites (1-dimensional interaction) and cubic lattice sites (3-dimensional interaction).

For an electrostatic interaction in linear and cubic lattice sites, the following equations may be obtained by applying the same assumptions:

$$E = E'_0 - \frac{RT}{F} \left\{ 2 \ln \frac{y}{1-y} + \frac{u}{kT} y \right\} \quad (10)$$

for an electrostatic interaction in linear lattice sites, which may correspond to an interaction in a 1-dimensional tunnel, and

$$E = E'_0 - \frac{RT}{F} \left\{ 2 \ln \frac{y}{1-y} + \frac{u}{kT} y^{1/3} \right\} \quad (11)$$

for an electrostatic interaction in cubic lattice sites.

Remaining problems, such as the physical meaning of the  $E_0$ s in eqns. (9), (10) and (11), and a possible refinement of those equations involving how the partition function can be modified to consider more general cases (including a thermodynamically "two phase" reaction with topotactic lithium insertion into a solid matrix [14]), will be discussed in a future paper, together with the experimental and analytical results of studies of metal oxide electrode systems.

## Acknowledgement

The present work was supported by the Aids for Scientific Research Programme of the Ministry of Education, Science and Culture, and by Asahi Glass Gijutsu Shoreikai.

## References

- 1 B. Reichman and A. J. Bard, *J. Electrochem. Soc.*, 128 (1981) 344.
- 2 N. Kumagai and K. Tanno, *Denki Kagaku*, 50 (1982) 704.
- 3 T. Ohzuku, K. Sawai and T. Hirai, *J. Electrochem. Soc.*, 132 (1985) 2828.
- 4 T. Ohzuku, T. Kodama and T. Hirai, *J. Power Sources*, 14 (1985) 153.
- 5 H. Schäfer, R. Gruehn and F. Schulte, *Angew. Chem.*, 5 (1966) 40, and references therein.
- 6 N. Terao, *Jpn. J. Appl. Phys.*, 2 (1963) 156.
- 7 G. Brauer, *Z. Anorg. Allg. Chem.*, 248 (1941) 1.
- 8 J. L. Waring, R. S. Roth and H. S. Parker, *J. Res. Nat. Bur. Stand. (U.S.A.)*, 77A (1973) 705.
- 9 K. Kato, *Acta Crystallogr.*, B32 (1976) 764.
- 10 W. Mertin, S. Anderson and R. Gruehn, *J. Solid State Chem.*, 1 (1970) 419.
- 11 N. C. Stephenson and R. S. Roth, *Acta Crystallogr.*, B27 (1971) 1018.
- 12 R. Kubo, *Tokeirikigaku (Statistical Thermodynamics)*, Kyoritsu Shuppan Co., Ltd., Tokyo, 1971.
- 13 R. H. Fowler and E. A. Guggenheim, *Statistical Thermodynamics*, Cambridge University Press, Cambridge, U.K., 1939, Ch. 2, 6, and 13.
- 14 T. Ohzuku, Y. Kogo and T. Hirai, *Manganese Dioxide Symp.*, 3 (1985) 391.